FIELD PILE LOAD TEST IN SALINE PERMAFROST

PART II

ANALYSIS OF RESULTS

by

K.W. Biggar[1] and D.C. Sego[2]

[1] Lecturer
Dept. of Civil Engineering
Royal Military College of Canada
Kingston, Ontario
K7K 5L0

[2] Professor of Civil Engineering
Department of Civil Engineering
University of Alberta
Edmonton, Alberta
T6G 2G7

Submitted to
Canadian Geotechnical Journal

August, 1991

ABSTRACT

The results obtained from 13 pile load tests carried out in saline permafrost at Iqaluit, N.W.T. are analyzed. This is the second paper that describes this study. The analysis examines:

- the performance of grout as a backfill material,
- the development of load along the length of the piles as determined from the strain gauge mounted along the embeded portion of the pile, and
- the time dependent deformation of the piles under load.

The grout used as backfill cured adequately and provided sufficient bond between the anchor and the grout to cause either the anchor to yield or the frozen soil which surrounded the grout to fail. The development of load along the pile results in a nearly uniform stress distribution for smooth piles but is highly non uniform if lugs are added to the pile.

The time dependent deformation of the piles without lugs can be described using a power law relationship.

Keywords: permafrost, saline, pile, load test, field, in-situ capacity, load transfer

Introduction

A field pile test program was conducted in Iqaluit, N.W.T. in 1988 by the University of Alberta (U of A) for the Department of National Defence (DND) to examine the performance of different pile configurations in saline permafrost and frozen rock, for foundation design guidance during the construction of the Short Range Radar (SRR) facilities. The preliminary presentation of the load versus displacement results in both the saline permafrost and rock were presented in Biggar and Sego (1989). A more detailed discussion of the factors influencing the performance of the piles, and a review of the site conditions, installation and testing procedures, and the load versus displacement results are contained in Part I of this paper (Biggar and Sego in press a) .

The intent of this paper is to provide additional test results data, and a detailed analysis thereof, pertaining to:

1. the performance of the grout which was used as a backfill material,

2. the development of load along the embedment of the piles as determined from strain gauges mounted along the pile length, and

3. the time dependent displacement behaviour of the piles, and

Performance of a high alumina cement grout backfill

General

A high alumina cement (Ciment Fondu) based grout was used as a backfill material for four anchors, two each with a neat grout (cement and water only) and a sanded grout (cement, sand, and water). The respective mix designs, by weight, were a water:cement

ratio of 0.35:1.0 , and a sand:water:cement ratio of 0.45:0.35:1.0. A powdered sulphonated napthelene formaldehyde condensate superplasticizer was utilized, in a proportion of 0.75% by weight of cement, to make the grout less viscous in order to ease placement. However it also had the effect of retarding the set time. The grout temperature was typically 25° to 30° C when it was placed. Anchor installation was accomplished by first pouring the grout into the hole to the desired depth, then lowering the Dywidag bar into the grout and aligning the bar with the assistance of the drill rig.

Thermal performance

Resistance temperatures devices (RTD's) were placed in the grout as close to the borehole wall as possible to measure the temperature of the grout as it cured, as shown in Figure 1. A typical plot of temperature versus time is shown in Figure 2. Generally the temperature of the grout decreased for approximately 4 hours then, as the grout hydrated, heat was generated and the temperature of the grout increased. Hydration was complete after approximately 8 hours and the temperature of the grout decreased until it stabilized at the temperature of the surrounding native soil, approximately 60 hours after placement. Curing of the grout was essentially complete after the temperature peaked, approximately 8 hours after mixing. Pertinent details of each test are contained in Table.1.

The minimum temperatures listed in Table 1 show that except in test #4 the grout adjacent to the native soil was subjected to sub-zero temperatures during the initial 10 hours, which would result in freezing of the mix water before curing of the grout was complete. As discussed in Biggar and Sego (1990) this results in a weaker grout, though its strength likely exceeded that of the surrounding permafrost.

The measured temperatures in pile #4 show that considerably greater amounts of heat were generated by the additional cement in the mix when a neat grout was used. Thus the use of neat grout in a 165 mm diameter hole in ice-rich or warm permafrost (T > -2° C) may

result in excessive thermal disturbance to the surrounding native soil. In the ice-poor till in which this test was conducted, however, no undesirable effects were observed.

Grout strength

Laboratory tests conducted with Dywidag bars embedded in properly cured Cement Fondu grout (Kast and Skermer 1986, and Biggar and Sego in press b,) indicate that the bond strength between the grout and the bar ranges between 4 and 7 MPa. Load tests were conducted approximately 6 weeks after pile installation so the grout strength was fully developed. An average bond strength of 2.8 MPa was obtained in a pullout test of a Dywidag bar grouted into rock at a nearby site in this test program (Biggar and Sego 1989), however the localized stress where the bar entered the grout may have been considerably greater. RTD readings from the tests in rock indicated that some of the grout adjacent to the rock may have been subject to freezing, but the grout adjacent to the bar is believed not to have frozen. Inspection of the anchors in rock was not possible so this could not be confirmed.

The compressive strength of Ciment Fondu grout in which the mix water has been subject to freezing during curing, when tested at temperatures above 0° C, is lower than for grout which has not experienced any freezing (Biggar and Sego 1990). No strength data is available, however, for grout which is maintained at sub-zero temperatures. The pile load tests conducted in this program indicate that the shear strength of the grout (in which the water was subject to freezing) exceeded the shear strength of the native soil (500 to 600 kPa), but since the actual failure surface along the embedded portion of the pile could not be examined this cannot be proven categorically.

Development of load at depth along the pile embedment

General

The development of load along the length of the pile was calculated from elastic analysis using the strain gauge data and the relationship:

$$P_i = \sigma_i A_x = (\varepsilon_i - \varepsilon_{io}) E A_x \quad (1)$$

where P_i denotes the load at the i^{th} strain gauge elevation, σ the axial stress, A_x denotes the cross sectional area of steel in the pile, ε the axial strain (measured) with the subscript 'o' denoting the strain gauge reading immediately prior to loading, and E is Young's Modulus for the pile material. The calculated shear stress over a portion of the pile was simply the change in the calculated load divided by the pile surface area between strain gauges at different elevations, expressed as:

$$\tau = \frac{\partial P}{\partial A_s} = \frac{(P_i - P_{i+1})}{\pi d (D_{i+1} - D_i)} \quad (2)$$

where A_S denotes the surface area of the pile, D the depth as a positive value, and d the pile diameter. Hence a linear load distribution indicates a uniform stress distribution, and a non-linear load distribution indicates a non-uniform stress distribution.

Redistribution of stress with time along the pile embedment in frozen soil is discussed in detail by Johnston and Ladanyi (1972), Nixon and McRoberts (1976), Weaver (1979), and Theriault and Ladanyi (1988). Generally uniform stress conditions will be experienced with short rigid piles during short time intervals. For longer rigid piles at relatively high loads or for more compressible piles (ie. timber) the stress distribution will be non-uniform initially, tending to become uniform as time progresses, examples of which are illustrated in Dipasquale et al. (1983) and Zhigul'skiy (1966). Long piles at relatively low loads may

never redistribute the stresses to the lower regions of the pile. The above is illustrated in Figure 3, from Linnel and Lobacz (1980).

The development and redistribution of load at depth for each of the pile configurations tested during the 1988 Iqaluit field program is discussed below. The term effective embedment refers to the portion of the pile below a depth of 4.0 m, which did not have any bond breaker material applied to the pile surface. The term applied load refers to the load applied at the top of the pile by the jack as measured by the load cell.

The calculation of shear stresses from the strain gauge data was complicated by two phenomena. The strain gauge cables were fastened to the pile surface, hence the surface area of the pile carrying the load was reduced by an amount equivalent to the area covered by the cables. Values of calculated shear stresses which have included a correction for this reduced surface area are listed in Table 2. Further, the HSS piles were installed with the bottom end open and the pile center was backfilled with dry sand. It is reasonable to assume that water from the slurry in the annulus between the pile and the native soil seeped into the centre of the pile although the actual height of rise of this water is unknown. Thus there would be a nominal force resisting the uplift force on the pile base equal to the lesser value of:

1. the area of the frozen soil in contact with the pile surface inside the pipe multiplied by the adfreeze bond strength; or

2. the cross-sectional area of the inside of the pile multiplied by the short-term tensile strength of the backfill material.

Analysis indicates that the maximum value of this force will be approximately 6 kN, beyond which the tensile strength of the backfill will be exceeded and the bond would rupture.

Smooth HSS pile with sand slurry backfill (#11)

Smooth HSS pipe with a sand backfill is similar to the pile configuration used for most adfreeze piles installed in permafrost. The load distribution along the pile embedment is shown in Figure 4. Little load was carried over the upper 3 m of the pile; a result of an active layer depth of approximately 1.5 m, warm soil temperatures from 1.5 to 3 m, and the bond breaker material applied to the pile surface. At small applied loads, a considerable portion of the load was resisted between 3 and 4 m even though the bond breaker had been installed along this portion. As the applied load increased, the resistance over this region decreased relative to the load carried over the effective embedment of the pile. The load versus depth relationship from 4 to 5.25 m was nearly linear indicating a uniform stress distribution along this region of the pile. The decrease in the slope of the load versus depth relationship between 5.25 and 6.5 m, at the bottom of the pile, suggests an increase in stress along this portion. Such behaviour is unlikely, and may be attributed to the effect of frozen material in the center of the pile as previously discussed. At applied loads of 70 and 80 kN there were anomalous strain gauge readings suggesting either strain gauge malfunction or localized failure of the adfreeze bond along the pile.

A linear least squares regression was performed on the load versus depth data for the portion of the pile between 4 and 5.25 m to estimate the in-situ uniform adfreeeze shear stresses on the pile. Shear stresses calculated by dividing the load applied at the top of the pile over the effective embedment of the pile are approximately 25% greater than shear stresses calculated from the strain gauge data (Table 2). Assuming that similar behaviour occurred for all smooth HSS and plain pipe piles, the *mobilized* adfreeze bond stresses at failure were approximately 50 to 70 kPa for smooth HSS and plain pipe piles.

The redistribution of load with time along the pile embedment is shown in Figure 5. Although the response measured by the strain gauges is not ideal, certain trends may be

observed. At a depth of 3 m where the bond breaker was applied there is little variation in the measured load with time. The measured load at the top of the effective embedment at a depth of 4.0 m, however, decreases as time progresses under the higher applied load increments. Conversely at a depth of 5.25 m a slight increase in the measured load is evident under the 80 kN load increment. Despite the small changes in measured load with time, the load distribution at the end of each load increment is nearly linear between the depths of 4 to 5.25 m as shown in Figure 4. At the failure load of 80 kN, the load measured at the 4.0 and 4.5 m depths converge to the same value indicating a failure of the adfreeze bond along this region of the pile.

The results from the strain gauges mounted at the 6.25 m depth are curious. It is uncertain whether the decrease in measured load is due to failure of the anchoring effect of frozen soil inside the pile as discussed above, a malfunction of the strain gauges, or a combination of the two.

Lugged HSS pile with sand slurry backfill (#12)

The load distribution along the embedment section of the pile, shown in Figure 6, is nearly linear for applied loads of 50 and 100 kN indicating a nearly uniform stress distribution, with provisions as noted previously for measured loads at 3 and 6.25 m. At the failure load of 150 kN the adfreeze bond stresses along the effective embedment of the pile above the lugs were approximately 50 kPa, shown in Table 2. After a short period of time the bond failed and the entire load was carried by the lugged portion of the pile, shown in Figure 6.

The load measured just below the lugs, at 6.25 m, was 30 kN at an applied load of 100 kN. Assuming a downward acting force on the bottom of the pile of 6 kN caused by the frozen soil inside the pile as detailed previously, it follows that the bond stresses along the lower 0.25 m of the pile were 468 kPa. Such a large adfreeze bond strength is unlikely

based upon the test results, hence either all three strain gauges at that depth had malfunctioned or the mechanism of load transfer at the bottom of the pile is much more complex than assumed in this analysis.

The load carried by the lugs on the pile can be considered as an equivalent stress carried over the 1 m portion onto which they were installed, or as a load per lug. According to the strain gauge data the load carried by the lugged portion of the pile was approximately 60 kN under an applied load of 100 kN, and approximately 120 kN under the failure load of 150 kN. In terms of an equivalent stress, the pile was stable at an equivalent stress of 60 kPa and failed at an equivalent stress of 120 kPa. Alternatively, in terms of a load per lug, the pile was stable at 15 kN per lug and failed at 30 kN per lug. Since the displacement rate of the pile only slightly exceeded the allowable rate at an applied load of 150 kN, it is reasonable to assume that the equivalent strength of the lugged portion pile was approximatley 100 kPa, or 25 kN per lug.

A reduction in load with time at a depth of 4.0 m, and a gain in load with time at 5.25 m is shown in Figure 7. The magnitude of the change in load was greater for the lugged pile than for the smooth HSS pile, due in part to the higher applied loads. The loads measured between 4.0 and 5.25 m converge to the same value at 360 minutes indicating that the adfreeze bond had completely failed at this time. The anomalously low value of load at 4.0 m depth beyond this time is assumed to be equipment error. As mentioned above, the results from the strain gauges at a depth of 6.25 m are unusual and no explanation has been determined for this behaviour.

Dywidag bar anchor with grout backfill (#3)

The load distribution along the embedded section of the Dywidag bar embedded in grout is shown in Figure 8 . Two major differences in behaviour, compared to the pipe piles, are evident: the load versus depth relationship was non-linear at all loads, and the

applied loads were much greater. Strain gauge output was only recorded at the end of each load increment, so no data is available regarding the redistribution of load with time along the bar.

The parabolic shape of the load versus depth relationship indicates a non-uniform shear stress distribution. Such a load distribution is common for Dywidag bars grouted into soil (Gaffran 1989; and Kast 1991) and is similar to that observed for deformed bars in concrete (Comite Euro-International du Beton 1982). The difference in the load versus depth distribution between the smooth piles and the Dywidag bar is a result of the radial stresses induced in the grout by the deformations on the surface of the bar as the anchor was loaded.

At an applied load of 575 kN (the load increment prior to failure), based upon the strain gauge data, the calculated average shear stress over the portion of the bar between the depths of 4.0 and 5.0 m was 559 kPa at the grout/native soil interface and 1921 kPa at the bar/grout interface. This compares to average stresses over the entire 2.5 m effective embedment of 417 kPa and 1430 kPa respectively. Examination of the strength of the different components of the anchor system shows:

1. unconfined compression tests conducted on core samples from the Iqaluit site tested at a strain rate of 0.8 %/hr and a temperature of -5° C gave shear strengths of 500 to 600 kPa,

2. the strength of the bond between the grout and the bar exceeded 2800 kPa at failure for tests of Dywidag bars grouted into rock at a nearby site (Biggar and Sego 1989), and

3. the yield strength of #14 Dywidag bars is 600 kN.

The results in Table 1 of Part I (Biggar and Sego in press a) show that all anchors were at or near their yield capacity, and the results from the strain gauged bar shows that the native soil was at or near failure in shear. The results from tests #3, #4 and #6 in which the anchors were unable to sustain the final load increment indicate that possibly the bars had also reached their yield point. Failure of the bars at loads less than 600 kN may have resulted if the anchors which were not vertically aligned when they were installed (ie. bending was also induced). It is possible, however, that for the grouted bars with failure loads less than 600 kN, the failure mechanism involved was one of shear failure of the native soil at the grout/native soil interface along the upper portion of the anchor, and the progression of this failure along the length of the pile. In this case the shear strength of the native soil was not fully developed along the entire length of the pile due to the non-uniform stress distribution. Because the failure surface was not examined it is not possible to ascertain which of the above failure mechanisms was invoked.

Due to the magnitude of the calculated load at the deepest strain gauges it again appears that there is an increase in shear stresses over the bottom 0.5 m of the pile. Such behaviour is unlikely hence the actual mechanism for the development of shear stress distribution at the base of the anchor is likely more complex than simply the shearing of concentric cylinders. Detailed analysis of such a mechanism is beyond the scope of this paper.

In summary, the adfreeze bond strength along the effective embedment of untreated piles was observed, from the strain gauge results, to be approximatley 50 to 70 kPa, or 25% less than that calculated using the load applied at the top of the pile. The lugged piles carried the load along the lugged portion of the piles after the adfreeze bond along the upper portion of the piles was exceeded (at approximatley 50 kPa). The equivalent strength along the lugged portion of the pile was approximatley 100 kPa, or 25 kN/lug. The stress

distribution along the effective embedment of the grouted anchors was non-uniform, and the failure mechanism was either one of yield of the bar or shear failure of the native soil commencing at the top of the effective embedment and progressing downwards. The calculated stresses at the bottom of the piles and anchor suggest that the localized load transfer mechanism was more complex than the shearing of concentric cylinders, however more research is necessary to better define the actual process involved. Finally at loads less than the failure load there was little redistribution of load along the depth of the pile with time, thus for practical purposes the stress distribution for smooth HSS piles was uniform at the end of each load increment. At the failure load, redistribution of load was observed, leading to the progressive failure of the adfreeze bond.

Time dependent pile displacement

The time dependent displacement of the different pile configurations has been analysed based on the following assumptions:

1. uniform stress distribution along the pile, and

2. the response of the pile at a given load increment is independent of previous load increments.

The first assumption has been shown to be valid for Smooth HSS piles and for lugged piles at loads less than 100 kN. Because the sandblasted piles had a planar surface similar to the Smooth HSS piles it is reasonable to assume that this assumption also applies to them. The first assumption has been shown to be invalid for grouted piles, and lugged piles at loads in excess of 150 kN.

The second assumption relates to the concept of hereditary creep in frozen soils, proposed in Ladanyi (1972), which is valid for non-strain strengthening materials. The

unconfined compression tests on the Iqaluit core samples showed the frozen soil was non-strain strengthening hence the assumption of hereditary creep is reasonable.

An equation proposed for the primary creep of piles in ice-poor soils by Weaver and Morgenstern (1981), based on earlier work by Vyalov (1959), Sayles (1968), Sayles and Haines (1974), and Johnston and Ladanyi (1972) is expressed as:

$$\frac{u_a}{a} = \frac{3^{(c+1)/2} D \tau^c t^b}{c - 1} \qquad (3)$$

where u_a = pile displacement

a = pile radius

D = experimentally determined temperature dependent coefficient

τ = applied shear stress

t = elapsed time

c = experimentally determined stress exponent

b = experimentally determined time exponent

For the conditions of constant temperature, stress and pile diameter, (3) reduces to:

$$u_a = K\ t^b \qquad (4)$$

where

$$K = \frac{3^{(c+1)/2} a D \tau^c}{(c - 1)} \qquad (5)$$

The parameters K and b may be determined for each load increment by plotting the pile displacement versus time using logarithmic coordinates. Using the average value of b for a

particular pile type and a least squares fit to the recorded data, the respective value of K for each load increment may be calculated. The recalculated values of K may then be plotted against the shear stress on logarithmic coordinates and the stress exponent, c, can be obtained. Substituting the value of c into (5) the respective value of D may be calculated. A typical example of this technique is shown in Figures 9 and 10.

The above procedure was applied to the results from the smooth HSS, lugged HSS, plain pipe, and sandblasted piles . Due to a scarcity of data for the smooth HSS and plain pipe piles, the results from the failure load increments were used, including only the values which represented an attenuating displacement rate. The calculated values of K and b for the tests are contained in Table 3. The initial values of b obtained from each load increment for the different pile configurations suggest that b is independent of the applied stress level but does depend on the pile surface conditions. The calculated pile displacement versus time based on the average b and recalculated K values is compared to the measured data in Figure 11a, 11b, and 11c for the Smooth HSS, Plain Pipe and Sandblasted Pipe piles respectively.

The values of c and D for the smooth HSS and plain pipe piles are not useful because of the lack of data at loads less than the failure load. In addition, for the Smooth HSS pile, there is a poor fit of the data to a linear least squares regression ($R^2 = 0.535$), and the calculated value of c, based on the three available data points, is less than unity, which is precluded by the formulation in equation (3).

The non-uniform shear stress distribution over the effective embedment of the grouted anchors negates the use of the above procedure to analyse the displacement versus time behaviour. Redistribution of stress along the length of the pile with time results in greater displacement rates than those applicable for uniform stress conditions, which may be observed in the results presented in Black and Thomas (1979). This is further illustrated

by applying the relationship expressed in equation (3) to the data from the grouted anchors; the values of K and b are listed in Table 3. As the applied load was increased the stress distribution became more uniform, shown in Figure 8, and the value of b decreased. Lower values of b (for more uniform stress conditions) will result in lower displacement rates and smaller displacements, as expected. The values of b at the highest load increments (hence the most uniform shear stress conditions) are approximately 1/3 as large as the values for the sandblasted piles. This suggests that after uniform stress conditions are attained for grouted anchors, the time dependent displacements will be smaller, and the displacement rates will be less than for sandblasted piles.

Comparison with results from others

A summary of published comparative pile load test data has been compiled in Table 4, listing both field and laboratory test data for each different pile configuration. It is apparent that there are considerable data available for piles with untreated surfaces but very little for the other configurations.

It must be noted that pile capacities in permafrost are also affected by relative strains between the pile and the frozen soil (Sanger 1969). Field pile load tests, however, generally only record pile head displacements, and detailed analysis is necessary to attempt to determine relative strains between the soil and the pile at depth. The following discussion deals only with adfreeze bond resistance or native soil shear strengths and does not attempt to concurrently analyse pile displacements.

Smooth HSS, and plain and sandblasted pipe

To enable the adfreeze bond strength values from tension tests to be comparable with compression test results it is reasonable to suggest that the values from the tension tests should be increased by 50% to 100%, as discussed in Part I (Biggar and Sego in press a) . Adjusting the values for the untreated piles in this study in such a manner gives adfreeze

bond values of approximately 100 to 150 kPa. Considering that the tests represent short term capacity, they are in reasonable agreement with the other field tests conducted in saline permafrost which were loaded for longer time intervals (Hoggan 1985; Nixon 1988; and Miller and Johnson 1990). The adfreeze bond strength results in saline permafrost are considerably lower than those reported in non-saline permafrost (Crory 1963; and Manikan, 1983).

No information was available dealing specifically with field load testing of sandblasted piles. Laboratory constant displacement rate tests on sandblasted piles have resulted in adfreeze bond strengths of 700 to 900 kPa in non-saline frozen sand (Parmeswaran, 1978, Sego and Smith, 1989, and Biggar and Sego, in press b, 670 kPa in a saline native soil with a clean sand backfill, and 390 kPa with a saline (10 ppt) silty sand backfill (Biggar and Sego in press b) . Constant load tests on sandblasted model piles in contact with saline soil resulted in adfreeze bond strengths of from 7 to 70 kPa at salinities of 15 and 5 ppt respectively (Hutchinson 1989).

The weak adfreeze bond strengths for sandblasted piles reported in Hutchinson (1989) suggest that there was no solute in contact with the piles in the present study. The results from Parmeswaran (1978), Sego and Smith (1989) and Biggar and Sego (in press b) however, suggest that the adfreeze strengths for the sandblasted piles were less than may be expected in a non-saline soil. This discrepancy may possibly be explained by the dependence of bond strength on relative strains between the pile and the soil, and that there were increased strains in the soil surrounding the pile during the field tests due to the salinity of the native soil.

Lugged HSS piles

Field test data for piles with protuberances on their surface is limited to those performed by the Alyeska Pipeline Co. presented in Black and Thomas (1979), Luscher et

al. (1983), and Ulrich et al. (1986), however the protuberances were over a much longer length of the pile, the load increment durations were 72 hrs, and they were compression tests performed in warmer, non-saline permafrost (-0.3° C). General comments on the performance of piles with protuberances are contained in Long (1973 and 1978). Thus direct comparison of the results from this study to other field test results is not possible. The general observations by these authors of shear failure occurring in the backfill material (or in the a weaker native soil) thereby providing pile load carrying capacity exceeding that governed by the adfreeze bond strength of the pile were also observed in the present study.

Laboratory tests on model piles with lugs, in frozen sand, conducted at displacement rates of 0.25 mm/hr, are reported in Andersland and Alwahhaab (1983). Enhanced load carrying capacities were observed with the introduction of lugs, and increased lug heights resulted in increased capacities, for lug heights between 1.59 and 4.76 mm. Interpolation from their results suggest that one 4.8 mm high lug in a non-saline sand at a temperature of -5.0° C would have a capacity of approximatley 13 kN. The values determined in this test program of approximatley 25 kN/lug for a 12 mm high lug are in general agreement with their observations. A fourfold increase in the capacity of aluminum model piles, when the piles were corrugated along their length, are reported in Ladanyi and Guichaoua (1985). Maximum shear stresses of approximately 250 kPa were observed for piles under constant load in a non-saline sand. For comparison purposes it is difficult to compensate for differences in scale, soil and pile physical properties, and load application, however the results from this study do show similar trends.

Grouted anchors

Detailed performance records of anchors grouted into permafrost are limited to those reported in Johnston and Ladanyi (1972), however soil temperatures in their tests were approximately -0.5° C. General comments about anchors grouted into frozen rock are contained in Kast and Skermer (1986), however no anchors were loaded to failure as the

capacity of the anchors exceeded the yield strength of the steel bars. A fourfold increase in ultimate adfreeze strength of cast-in-place concrete piles over slurry backfilled concrete piles in warm permafrost (-0.5° C) are reported by the Research group on pile foundations, People's Republic of China (1978), however details are lacking. No laboratory test results of grouted piles in frozen soil were found in the literature.

Although no quantitative comparisons are available, excavation of some anchors was undertaken in the study by Johnston and Ladanyi (1972). The surface of the grout was observed to be corrugated, following the contours left by the auger during drilling. The deformations in the surrounding soil consisted of a highly sheared thin zone immediately adjacent to the anchor associated with slip at the interface during failure, and an outer zone of uniform shear strain which decreased rapidly with distance from the anchor. Similar performance of the anchors in this study is expected.

Conclusions

The cement grout which was used as a backfill material for 48 mm diameter Dywidag bars in a 165 mm diameter hole provided sufficient strength to yield the steel bar (600 kN) and possibly caused shear failure within the native soil. The neat grout , however, resulted in considerably higher temperatures during curing. Consequently it is recommended that for similar installation conditions a sanded grout be utilized as it generates less heat during curing (hence less thermal disturbance to the surrounding permafrost), and less cement is required resulting in a less expensive mix.

The results from the strain gauge data showed a nearly uniform distribution of stress at the end of each load increment for the smooth HSS pile. The results also showed that the mobilized adfreeze shear stress was approximately 75% of the stress calculated by simply dividing the load applied at the top of the pile by the effective embedment area of the pile. The stress distribution was non-uniform for the lugged HSS pile at loads in excess of

100 kN, and for all load increments on the grouted anchor. This emphasizes that it is unconservative to expect to fully mobilize the shear strength of the soil along the entire pile length because a progressive failure will occur where failure of the soil at the upper regions of the pile occurs before the maximum stress is developed along the lower regions of the pile.

The initial time dependent deformation of the piles which had no protuberances on their surface can be described by a power law in the form:

$$u_a = K\ t^b$$

It is not possible to determine if the relationship will provide adequate results for long-term deformations since no long term load tests were conducted.

Recommendations for Future Research

There is still concern regarding the strength of grout in which the water has been subject to freezing during curing, and which remains frozen in the permafrost. One solution to the problem is to develop a grout, using suitable cement and admixtures, which will prevent the mix water from freezing. This is an expensive solution which requires careful control during mixing and installation, but one which has been recently addressed on several fronts (Biggar and Sego 1990; Ballivy et al. 1990; and Korhonen 1990). For piles and anchors grouted into permafrost *soils* it is possible that the strength of grout which has been subject to freezing exceeds that of the surrounding native soil such that the failure will still occur in the soil. The strength of grouts whose water has been subject to freezing, and which remain frozen, should be investigated to resolve a controversial construction problem and possibly result in less expensive grout mix designs.

The results from the strain gauge data indicate that the stress distribution at the base of the pile is more complex than generally assumed in design and analysis, and that enhanced

load carrying capacity is evident. If this is the case, marginal gains in pile capacity may be possible if the mechanism is better defined.

Long term load tests of piles in saline ice-poor permafrost will determine if a power law similar to the one proposed in this paper (for an attenuating pile displacement rate) is appropriate to estimate long-term deformations or whether a constant displacement rate formulation (Nixon 1988) is more suitable.

The issue of when it is economical to use grout backfilled piles in saline permafrost should be addressed. This includes the problems of solute migration into the slurry backfill, the long-term load carrying capacity of slurry backfilled piles in saline permafrost compared to grout backfilled piles, and the economics of purchasing, transporting and placing the grout.

References

Andersland, O.B., and Alwahhaab. M.R. 1983. Lug behavior for model steel piles in frozen sand. Proceedings, 4th International Conference on Permafrost, Fairbanks Alaska, USA. pp. 16-21.

Biggar, K.W. and Sego, D.C. 1989. Field load testing of various pile configurations is saline permafrost and seasonally frozen rock. 42nd Canadian Geotechnical Conference, October 25-27, Winnipeg, pp. 304-312.

Biggar, K.W., and Sego, D.C. 1990. The curing and strength characteristics of cold setting Ciment Fondu grout. Proceedings, 5th Canadian Permafrost Conference. Quebec City, Quebec, pp. 349-355.

Biggar, K.W. and Sego, D.C.,1991. in press a. Field pile load tests in saline permafrost, Part I, Procedures and results.

Biggar, K.W. and Sego, D.C. ,1991. in press b. Model adfreeze and grouted piles in saline permafrost, Part 2, Strength and deformation behaviour.

Biggar, K.W. and Sego, D.C., 1991. in press c. Model adfreeze and grouted piles in saline permafrost, Part 2, Time dependent displacement behaviour .

Black, W.T., and Thomas, H.P. 1979. Prototype pile tests in permafrost soils. in Pipelines in Adverse Environments: A State of the Art, Proceedings of the ASCE Pipeline Division Specialty Conference , New Orleans, Louisiana, **1**. pp. 372-383.

Comite Euro-International du Beton. 1982. Bond action and bond behaviour of reinforcement: State-of-the-art. Information Bulletin No 151, Contribution to the 22 Session Pienière du C.E.B., Munich, West Germany, pp. 20-49.

Crory, F.E. 1963. Pile foundations in permafrost. Proceedings, 1st International Conference on Permafrost, Lafayette, Indiana, USA. pp. 467-476.

DiPasquale, L., Gerlek, E., and Phukan, A. 1983. Design and construction of pile foundations in Yukon Kuskokwin Delta, Alaska. Proceedings, 4th International Conference on Permafrost, Fairbanks Alaska, USA, pp. 238-243

Gaffran, P. 1989. Monitoring of anchored sheet pile walls. Unpublished MSc Thesis, University of Alberta, p. 514.

Hivon, E.G. 1991. Behaviour of saline frozen soils. Unpublished Ph. D. thesis, University of Alberta, Edmonton, Alberta. p. 435.

Hoggan Engineering and Testing (1980) Ltd. 1985. Pile load tests, Arctic Bay multi-purpose Hall and School Extension, Report to Government of the North West Territories, Department of Public Works.

Hutchinson, D.J. 1989. Model pile load tests in frozen saline silty sand. Unpublished M.Sc. Thesis, University of Alberta, Edmonton, Alberta, p. 222.

Johnston, G.H., and Ladanyi, B. 1972. Field tests on grouted rod anchors in permafrost, Canadian Geotechnical Journal. **9**: 176-194.

Karpov, V., and Velli, Y. 1968. Displacement resistance of frozen saline soils. Soil Mechanics and Foundation Engineering (English Translation), **4** (July/August): 277-388.

Kast, G. and Skermer, N. 1986. DEW Line anchors in permafrost. Geotechnical News, **4** (4): 30-34.

Kast, G. 1991. Personal Communication. Vice President Western Division, Dywidag Systems International Canada Ltd (DSI).

Ladanyi, B. 1972. An engineering theory of creep in frozen soils. Canadian Geotechnical Journal, **9:** (1): 63-80.

Ladanyi, B., and Guichaoua, A. 1985. Bearing capacity and settlement of shaped piles in permafrost. Proceedings, XI International Conference on Soil Mechanics and Foundation Engineering, San Francisco, USA, pp. 1421-1427.

Linnell, K.A., and Lobacz, E.F. 1980. Design and construction of foundations in areas of deep seasonal frost and permafrost. US Army Cold Regions Research and Engineering Lab, Hanover, New, Hampshire, Special Report 80-34, p. 320.

Long, E.L. 1973. Designing friction piles for increased stability at lower installed cost in permafrost. Proceedings, 2nd International Conference on Permafrost, North American Contribution, Yakutsk, USSR, pp. 693-698.

Long, E.L. 1978. Permafrost Foundation Designs. Proceedings: Cold Regions Specialty Conference, Anchorage, Alaska, American Society of Civil Engineering, 17-19 May. 11, pp. 973-987

Luscher, U., Black, W.T., and McPhail, J.F. 1983. Results of load tests on temperature-controlled piles in permafrost, Proceedings, 4th International Conference on Permafrost, Fairbanks Alaska, USA, pp. 756-761.

Manikian, V. 1983 Pile driving and load tests in permafrost for the Kuparuk pipeline system. Proceedings, 4th International Conference on Permafrost, Fairbanks Alaska, USA, pp. 804-810.

Miller, D.L. and Johnson, L.A. 1990. Pile settlement in saline permafrost: a case history. Proceedings, 5th Canadian Permafrost Conference. Quebec City, Quebec. pp. 371-378.

Nixon, J.F., and McRoberts, E.C. 1976. A design approach for pile foundations in permafrost. Canadian Geotechnical Journal, **13**: 40-57.

Nixon, J.F. 1988. Pile load tests in saline permafrost at Clyde River, Northwest Territories, Canadian Geotechnical Journal, **25**: 24-31.

Parmeswaran, V.R. 1978. Adfreeze strength of frozen sand to model piles.Canadian Geotechnical Journal, **15**: 494-500.

Research Group on Pile Foundations in Permafrost, Research Institute of Ministry of Railways, The People's Republic of China. 1978. Testing of pile foundations in permafrost areas. Proceedings, 3rd International Conference on Permafrost, Edmonton, Alberta, Canada., **1.** pp. 179-185.

Sanger, F.J. 1969. Foundations of structures in cold regions. US Army Cold Regions Research and Engineering Laboratory, Hanover, New Hampshire, Monograph III-C4, p. 93.

Sayles, F.H. 1968. Creep of frozen sands. US Army Cold Regions Research and Engineering Laboratory, Hanover, New Hampshire, Technical Report 190, p. 54.

Sayles, F.H., and Haines, D. 1974. Creep of frozen silt and clay. US Army Cold Regions Research and Engineering Laboratory, Hanover, New Hampshire, Technical Report 252, p. 51.

Sego, D.C. and Smith, L.B. 1989. The effect of backfill properties and surface treatment on the capacity of adfreeze pipe piles. Canadian Geotechnical Journal, **26**: 718-725.

Theriault, A. and Ladanyi, B. 1988. Behaviour of long piles in permafrost. Proceedings, 5th International Conference on Permafrost, Trondheim, Norway. pp. 1175-1180.

Thomas, H.P., and Luscher, U. 1980. Improvement of bearing capacity of piles by corrugations. US Army Cold Regions Research and Engineering Laboratory, Hanover, New Hampshire, Special Report 80-40, pp. 229-234.

Ulrich, U., Black, W.T., and McPhail, J.F. 1986. Results of load tests on temperature-controlled piles in permafrost. Proceedings, 4th International Conference on Cold Regions Engineering, TCCRE, ASCE, Anchorage, Alaska, USA, pp. 756-761.

Vyalov, S.S. 1959. Rheological properties and bearing capacity of frozen soils. Translation 74, U.S. Army US Army Cold Regions Research and Engineering Laboratory, Hanover, New Hampshire, translated in 1965, p. 219.

Weaver, J.S. 1979. Pile foundations in permafrost. Unpublished Ph. D. thesis, University of Alberta, Edmonton, Alberta, p. 224.

Weaver, J.S., and Morgenstern, N.R. 1981. Pile design in permafrost. Canadian Geotechnical Journal, **18**: 357-370.

Zhigul'skiy, A.A. 1966. Experimental investigation of the state of stress and strain in the soil around a pile. Proceedings, 8th Conference on Geocryology, Yakutsk, USSR, Part 5, pp. 211-223.

List of Tables

List of Figures

TABLE 1

Iqaluit grout curing temperature details

Pile #	Grout Type	Minimum Temperature (°C)	Time to Min Temp (hrs)	Maximum Temperature (°C)	Time to Max Temp (hrs)	Comments
2	Neat	-1.2	5.0	6.9	11.3	1.0% SPN [1]
3	Sanded	-0.8	3.2	14.1	7.7	0.75% SPN
4	Neat	2.4	1.8	36.4	5.3	0.75% SPN
6	Sanded	-1.1	4.8	7.0	9.9	0.75% SPN

Note 1. Poor seal at bottom of casing allowed material to slough into the hole during grout placement

TABLE 2

Corrected shear stresses on strain gauged piles

Assuming a uniform stress distribution between 4.0 and 5.25 m depth, and performing a linear least squares regression on the calculated load versus depth data.

	Applied Load (kN)	Slope ($\Delta P/\Delta L$)	Stress [1] (kPa)	Stress [2] (kPa)	Stress [3] (kPa)
Smooth HSS	50	9.449	26	29	56
1-11	60	16.05	45	49	67
	70	19.85	55	60	78
Lugged HSS	50	7.453	21	23	56
1-12	100	14.45	40	44	112
	150 [4]	16.69	47	51	168

Notes:
[1] Calculated as: Slope ÷ (π d).
[2] Corrected for pile surface area covered by cables (weighted average of 8%).
[3] Average stress using applied load over embedment length.
[4] Used data from second time increment only as data at subsequent increments had anomalous values.

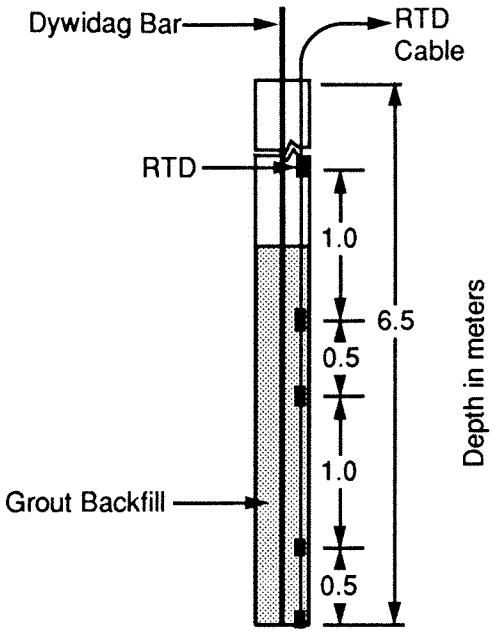

Figure 1: Location of RTD's to Measure Grout Curing Temperatures

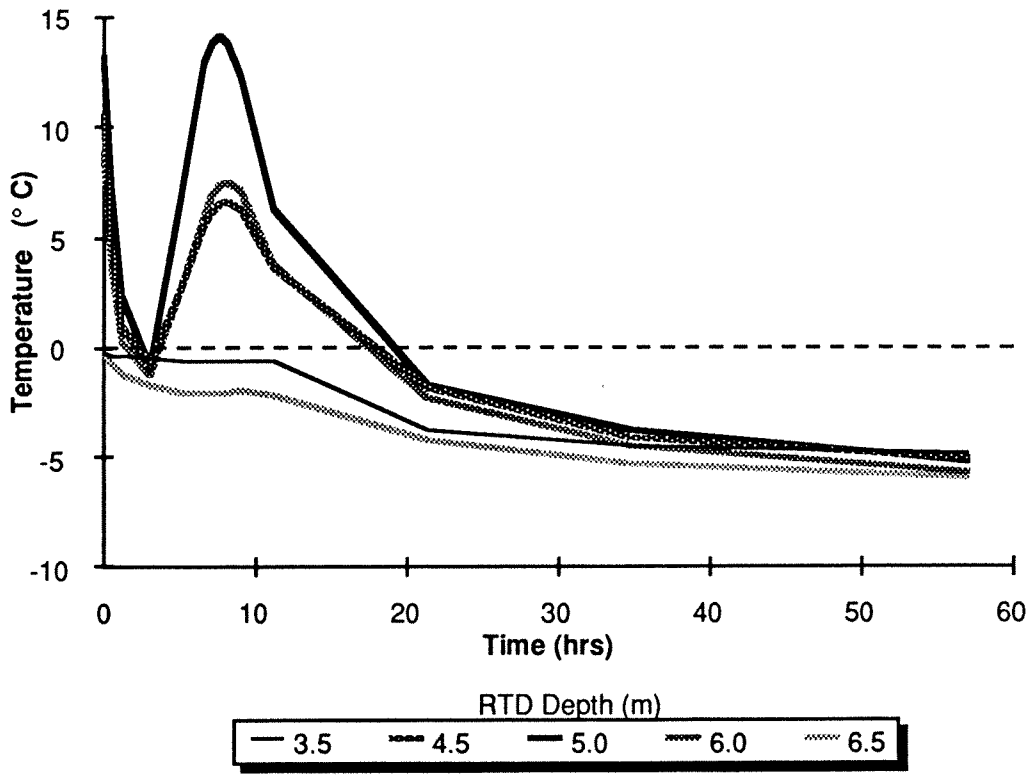

Figure 2: Temperature versus Time for Sanded Grout

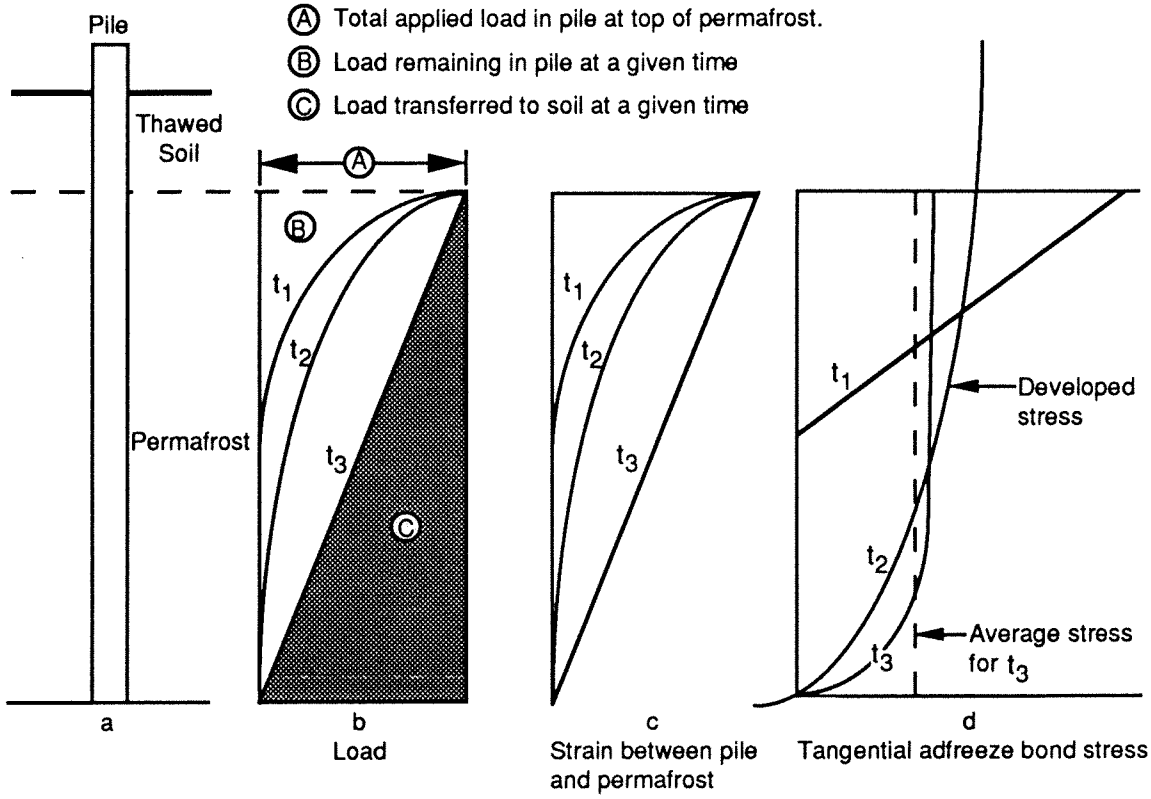
Ⓐ Total applied load in pile at top of permafrost.
Ⓑ Load remaining in pile at a given time
Ⓒ Load transferred to soil at a given time
Pile
Thawed Soil
Permafrost
Ⓐ
Ⓑ
Ⓒ
t_1
t_2
t_3
Developed stress
Average stress for t_3
a
b
Load
c
Strain between pile and permafrost
d
Tangential adfreeze bond stress

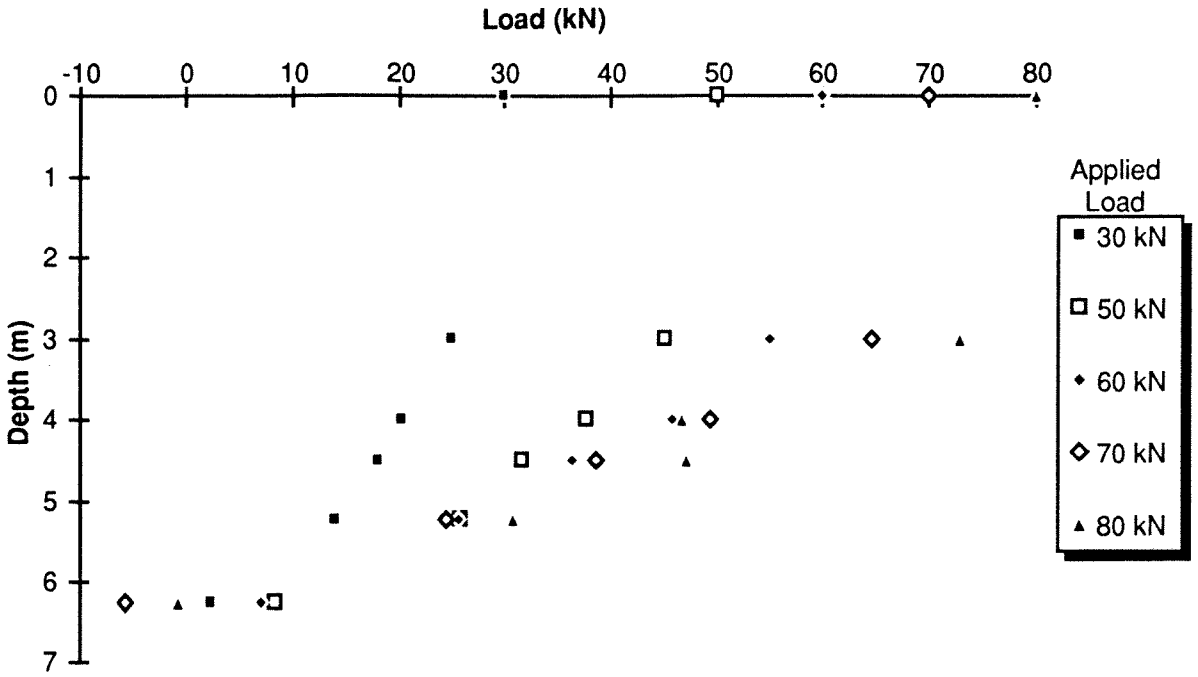

Figure 4: Smooth HSS Pile -Load at Depth for various load increments

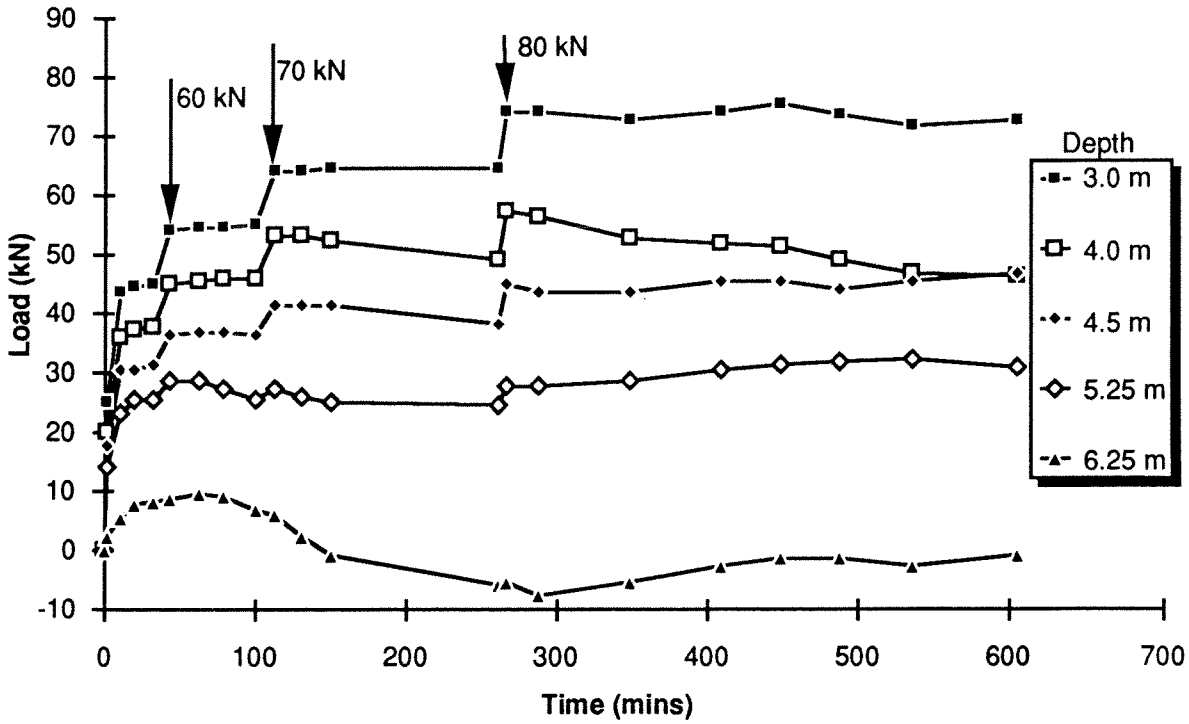

Figure 5: Smooth HSS Pile -Load at various Depths versus Time

TABLE 3
Results of displacement versus time analysis

Test #	Pile Type	Load (kN) Failure	Load (kN) Applied	Measured Values K (mm min)	Measured Values b	R for b	Average b	Recalc K (mm min)	Estimated Shear Stress* (kPa)	Calculated Values c	Calculated Values D (mm min kPa)	Calculated Values R for c
7	Smooth HSS	100	100	0.845	0.167	0.976	0.140	0.923	84			
11	Smooth HSS	70	60	0.646	0.128	0.973	0.140	0.644	50	0.581	0.0742	0.535
			70	0.980	0.124	0.936	0.140	0.931	59			
				Average =	0.1399							
15	Plain Pipe	80	75	1.52	0.0449	0.940	0.0573	1.49	63			
			80	1.69	0.0634	0.906	0.0573	1.78	67	1.07	0.0189	0.981
16	Plain Pipe	60	40	0.741	0.0635	0.904	0.0573	0.823	34			
				Average =	0.05727							
13	Sandblasted Pipe	290	170	2.26	0.0374	0.994	0.0491	2.22	142			
			210	2.93	0.0393	0.991	0.0491	2.88	176			
			250	3.86	0.0327	0.973	0.0491	3.70	209			
			270	4.28	0.0379	0.981	0.0491	4.17	226	1.51	0.00116	0.952
14	Sandblasted Pipe	250	180	1.85	0.0751	0.991	0.0491	2.06	151			
			210	2.45	0.0640	0.928	0.0491	2.64	176			
			230	3.07	0.0574	0.946	0.0491	3.21	193			
				Average =	0.04912							
12	Lugged HSS	150	50	0.361	0.189	0.978						
4	Neat Grout	620	250	4.97	0.0472	0.993						
			350	6.83	0.0450	0.997						
			450	9.57	0.0252	0.991						
			540	12.2	0.0176	0.962						
			580	13.9	0.0162	0.950						
6	Sanded Grout	570	250	6.18	0.0505	0.962						
			350	8.56	0.0392	0.992						
			450	10.7	0.0356	0.997						
			500	12.6	0.0228	0.993						
			540	14.0	0.0174	0.959						

* Estimated Shear stress calculated as: $\frac{0.75 \times \text{Applied Load}}{\text{Effective Embedment Area}}$

TABLE 4
Comparative test data

Author(s)	Native Soil [1]		Backfill [1]		Pile	Diameter	Temp	Failure Stress	Failure Time	Load or Displ	Load	Comments
	Material	S (ppt)	Material	S (ppt)	Surface [2]	(mm)	(°C)	(kPa)	(mins)	Rate	Type [3]	
SMOOTH PILE SURFACE												
Field Test Results												
Crory (1963)	?	0?	SM	0	Un	200	-3.3	325		45 kN /day	C	
Crory (1963)	?	0?	SP	0	Un	200	-2.2	~ 385		45 kN /day	C	
Manikian (1983)	SM [5]	0	SP	0	Un	457	-6.0	615	197	~ 3 kPa/min	T	
Hoggan (1985)	DS & S [4]	10-30	SP	0?	Un	114	~ -5	90		33 kN/day	C	
Miller et. al. (1990)	SM	20-60	SM	0	Un	457	~ -4	30-50		Const Load	C	Note 9.
Nixon (1988)	SM	15-30	SM	15-30	Un	140	~ -6	80		Const Load	C	
This study	SW [6]	15-25	SP	0	Un	114	-4.8	50-70 [7]	20-60 [8]	>.25 mm/hr	T	
This study	SW [6]	15-25	SP	0	Sb	114	-5.2	323	20-50 [8]	>.25 mm/hr	T	
Laboratory Test Results												
Ladanyi and Guichaoua (1985)	SP	0	SP	0	Un Al	20	-5.0	429	?	.062 mm /min	C	
Ladanyi and Guichaoua (1985)	SP	0	SP	0	Un Al	20	-5.0	62	7200	Const Load	C	
Parmeswaran (1978)	SP	0	SP	0	Sb	76	-6.0	800	185	.005 mm /min	C	
Parmeswaran (1978)	SP	0	SP	0	Sb & P	76	-6.0	677	110	.005 mm /min	C	
Karpov and Velli (1968)	CL	10	CL	10	Wood &	100	-4.5	660	?	150 kPa /min	C	Short-term
Karpov and Velli (1968)	CL	10	CL	10	Concrete	100	-4.5	170	?	Incremental	C	Long-term
Sego and Smith (1989)	SM	10	SP	0	Un	33	-5.0	360	120	.006 mm /min	C	
Sego and Smith (1989)	SM	10	SM	10	Un	33	-5.0	190	162	.006 mm /min	C	
Sego and Smith (1989)	SM	0	SP	0	Sb	33	-5.0	733	378	.006 mm /min	C	
Hutchinson (1989)	SM	0	SM	0	Sb	33	-5.0	193	~ 14000	Const Load	C	
Hutchinson (1989)	SM	5	SM	5	Sb	33	-5.0	71	100	Const Load	C	
Hutchinson (1989)	SM	15	SM	15	Sb	33	-5.0	7.5	250	Const Load	C	
Biggar and Sego (in press)	SM	0	SP	0	Sb	33	-5.0	887	160	.008 mm /min	C	
Biggar and Sego (in press)	SM	10	SP	0	Sb	33	-5.0	670	180	.008 mm /min	C	
Biggar and Sego (in press)	SM	10	SM	10	Sb	33	-5.0	126	55	.008 mm /min	C	
Biggar and Sego (in press)	SM	30	SM	30	Sb	33	-5.0	6	155	.008 mm /min	C	
RIBBED PILE SURFACE												
Field Test Results												
Luscher et al (1983)	ML [5]	0	SP	0	Cor	457	-0.3	200-275+	?	89 kN / 3 day	C	
Luscher et al (1983)	CL	0	SP	0	Cor	457	-0.3	120	?	89 kN / 3 day	C	
This study	SW [6]	15-25	SP	0	Lugged	114	-5.0	120		>.25 mm/hr	T	Excessive displacement rate
Laboratory Test Results												
Andersland and Alwahhab (1983)	SP	0	SP	0	1 Lug	9.5	-5.0	13 kN /lug		.25 mm /hr	T	Note 10.
Ladanyi and Guichaoua (1985)	SP	0	SP	0	Cor Al	22	-5.0	~ 250		Const Load	C	Min rate 0.004 mm /hr
Ladanyi and Guichaoua (1985)	SP	0	SP	0	Cor Al	22	-5.0	1790	~ 170	0.3 mm /min	C	
GROUTED ANCHORS												
Field Test Results												
Johnston and Ladanyi (1972)	CL [5]	0	Grout	N/A	Re bar	150	-0.5	249	<120	Const Load	T	Gillam results.
Johnston and Ladanyi (1972)	CL [5]	0	Grout	N/A	Re bar	150	-0.5	118	~ 75000	Const Load	T	Gillam results.
This study	SW [6]	15-25	Grout	0	Dywidag	165	-5.0	560		>.25 mm/hr	T	Unable to maintain last load increment

Notes: 1. Based on Unified Soil Classification system, S denotes salinity.
2. Pile surface treatment: Sb = sandblasted, Un = untreated, P = painted, Al = aluminum, Cor = corrugated.
3. Compression = C, Tension = T.
4. Dolomitic Shale and Slate, fissured with ice.
5. Ice-rich.
6. Dense clayey, gravelly sand with some cobbles, moisture content 6.5% to 9.5%.
7. Adjusted based on strain gauge results. Range of results from 4 tests.
8. Time to failure for last increment only.
9. Excessive settlement of pile foundation in summer.
10. For 4.8 mm lug, estimated based on data presented in paper.

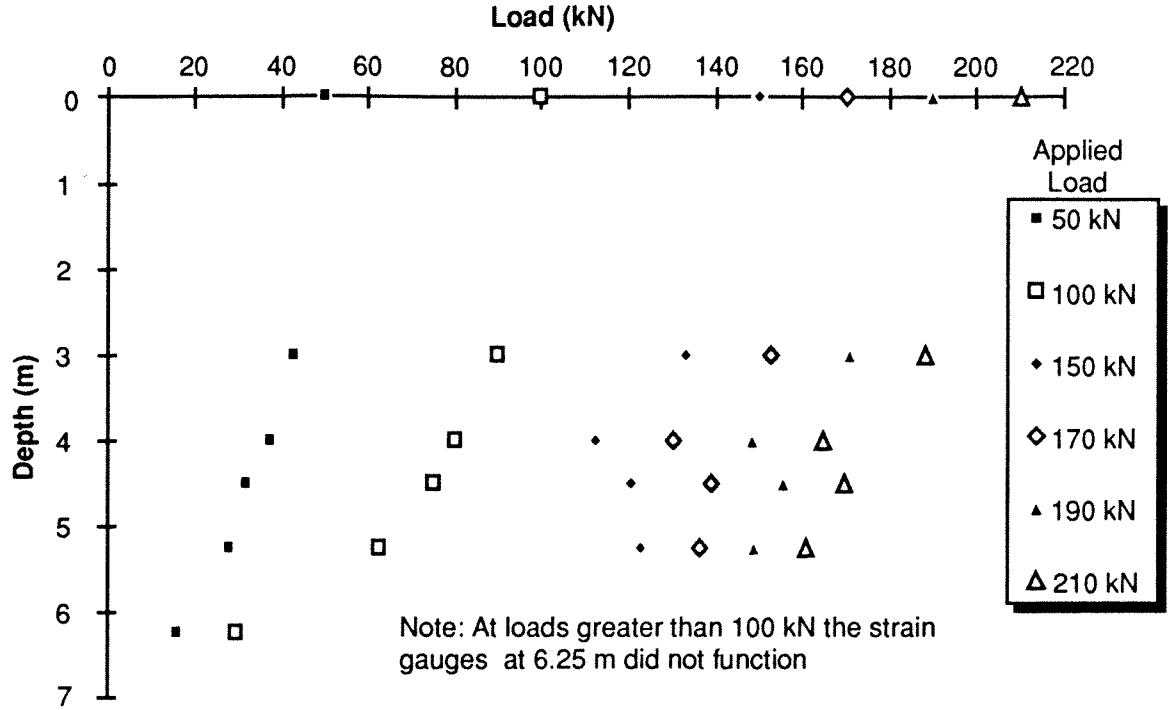

Figure 6: Lugged HSS Pile -Load at Depth for various load increments

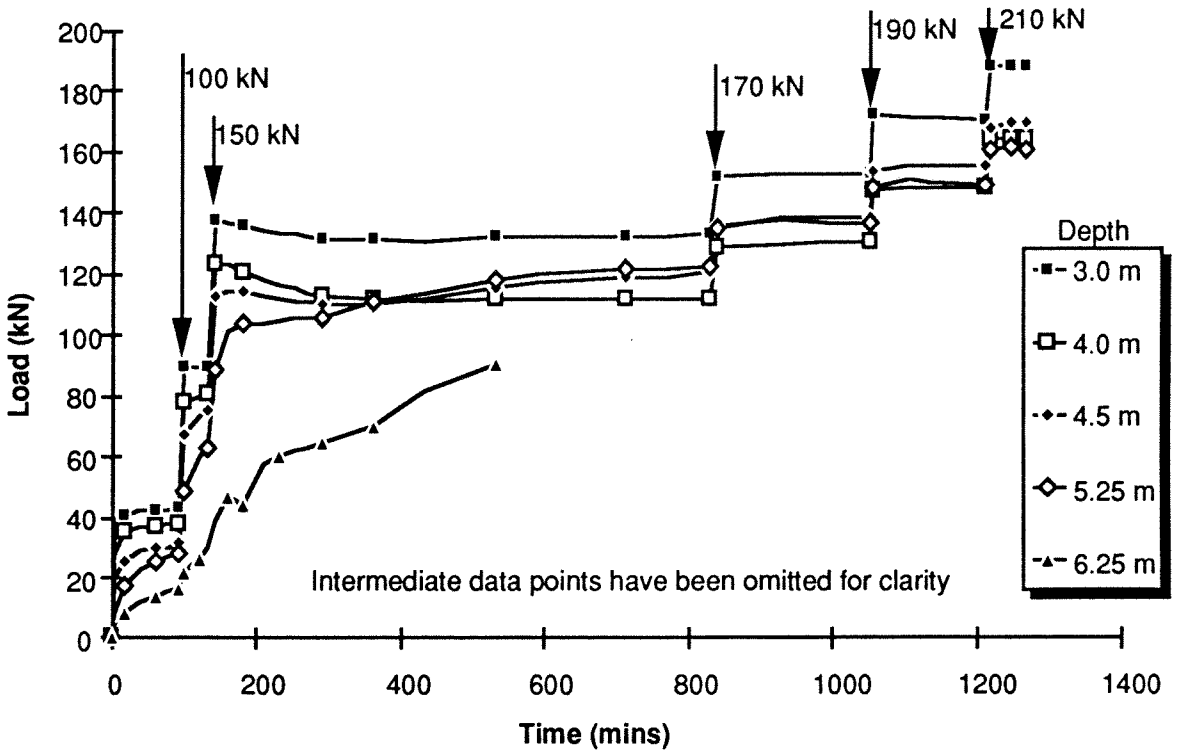

Figure 7: Lugged HSS Pile -Load at various Depths versus Time

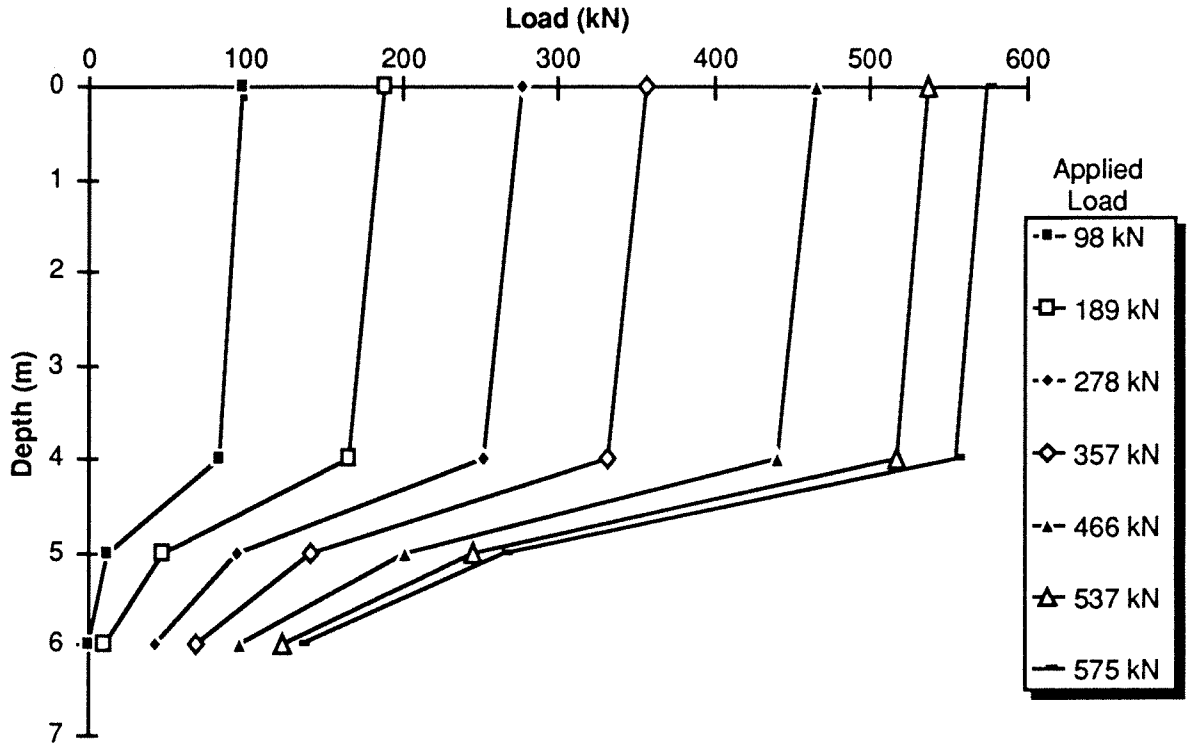

Figure 8: Dywidag bar -Load at Depth for various load increments

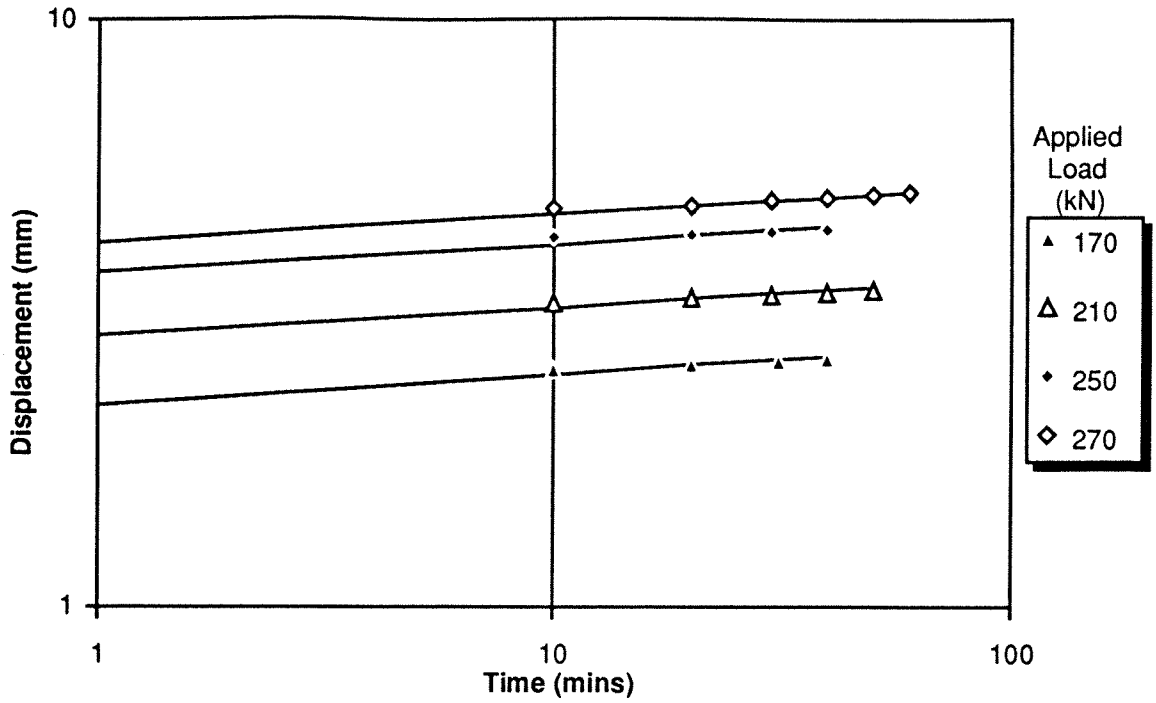

Figure 9: Typical Displacement versus Time - Measured values and best fit regression line

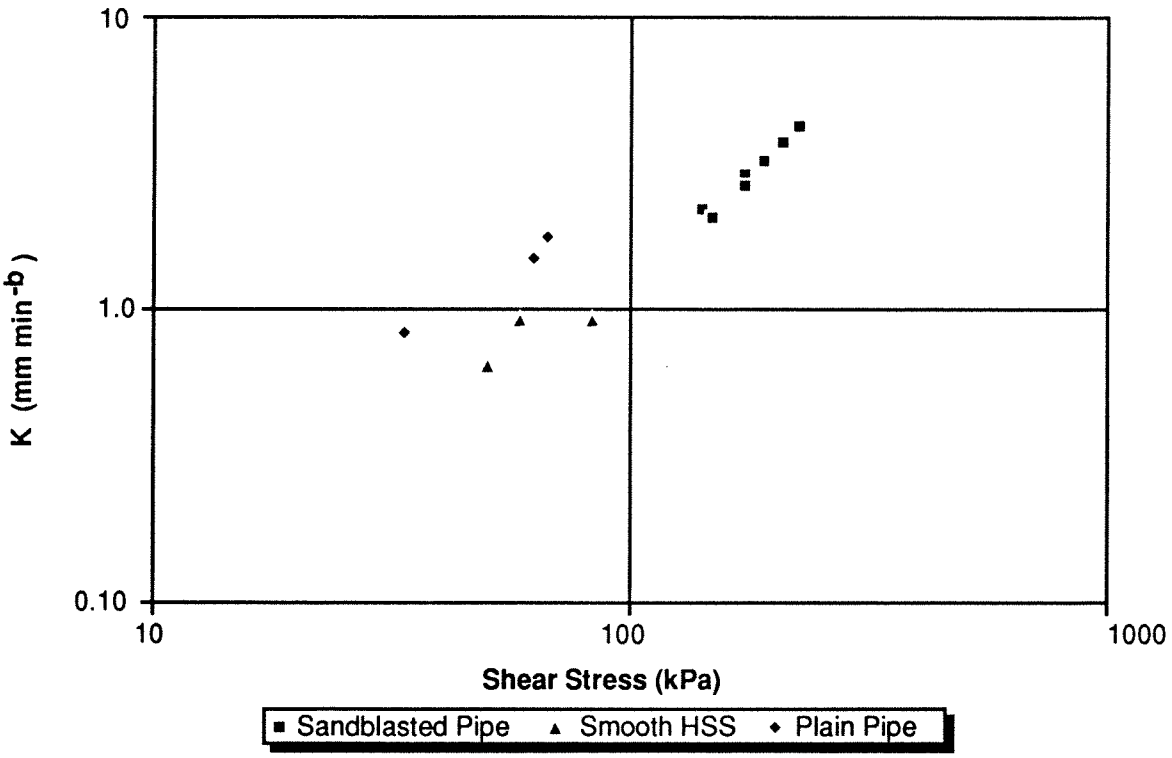

Figure 10: Values of K parameter versus Shear stress for different pile configurations

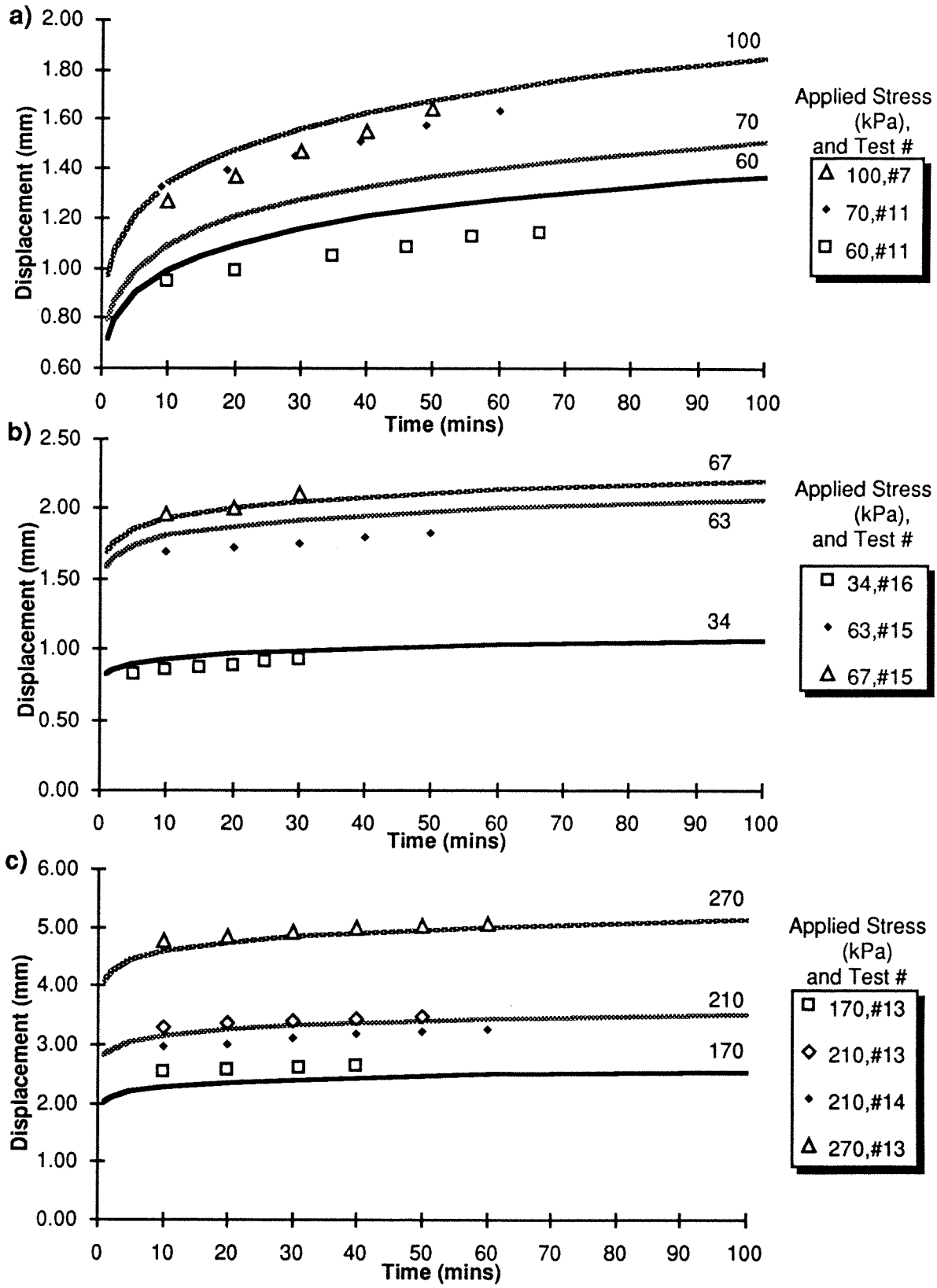

Figure 11: Displacement versus time–Predicted performance and measured values a)Smooth HSS b)Plain Pipe c)Sandblasted Pipe